

# Cellular automaton model for evacuation process with obstacles

A. Varas<sup>a</sup>, M.D. Cornejo<sup>a</sup>, D. Mainemer<sup>a</sup>, B. Toledo<sup>b,\*</sup>,  
J. Rogan<sup>a</sup>, V. Muñoz<sup>a</sup>, J.A. Valdivia<sup>a</sup>

<sup>a</sup>*Departamento de Física, Facultad de Ciencias, Universidad de Chile, Chile*

<sup>b</sup>*Departamento de Física, Universidad de Santiago de Chile (USACH), Chile*

Received 29 December 2006

Available online 19 April 2007

---

## Abstract

A bidimensional cellular automaton model is used to simulate the process of evacuation of pedestrians in a room with fixed obstacles. A floor field is defined so that moving to a cell with lower floor field means approaching an exit door. The model becomes non-deterministic by introducing a “panic” parameter, given by a probability of not moving, and by a random choice to resolve conflicts in the update of pedestrian positions. Two types of exit doors are considered: single (where only one person can pass) and double (two persons can pass simultaneously). For a double door, the longest evacuation time turns out to occur for a very traditional location of the door. The optimum door position is determined. Replacing the double door by two single doors does not improve evacuation times noticeably. On the other hand, for a room without obstacles, a simple scaling law is proposed to model the dependence of evacuation time with the number of persons and exit width. This model fails when obstacles are present, as their presence introduces local bottlenecks whose effect outweighs the benefits of increasing door width beyond a certain threshold.

© 2007 Elsevier B.V. All rights reserved.

**Keywords:** Pedestrian evacuation; Cellular automata

---

## 1. Introduction

Recent research has shown that complex behavior phenomena in traffic flows and pedestrian streams can be successfully studied from a physical viewpoint (see, e.g., Ref. [1] and references therein, [2–4]). Collective behaviors studied include jam formation, clogging, “faster-is-slower” effect, oscillation at doors and lane formation, among others [5–11]. Various scenarios have been considered, such as escape panic [12], evacuation in conditions of poor visibility [13], egress from aircraft [14], pedestrian counterflows [7,10,15,16], motion in T-shaped channels [9] or through bottlenecks [17], or the effects of kin behavior [18] and competitive/cooperative behavior [14]. Several models have been proposed to study these systems, including molecular dynamics [6,12], lattice gas [7,9,13,17,19,20] and cellular automata (CA) models [5,11,14–16,21–23]. CA models are a particularly interesting choice, since, in spite of its computational simplicity, they are able to

---

\*Corresponding author. Tel.: +56 2 7763322.

E-mail address: [btoledo@fisica.ciencias.uchile.cl](mailto:btoledo@fisica.ciencias.uchile.cl) (B. Toledo).

model individual and collective behavior of pedestrian dynamics observed experimentally and described by other, more complex models [5,11,14,22,23].

A particularly interesting problem is motion in a room with obstacles. This is of primary importance, as many real situations of emergency evacuations occur in such rooms, like movie theaters, aircrafts, classrooms, etc. Also if panic is involved, pedestrians may fall and become obstacles to other pedestrians. In spite of its importance, relatively few research has been devoted to this problem [5,19,24]. A relevant problem in this regard is how to distribute exits or obstacles in a room in order to improve evacuation times. Some aspects of this problem have been studied using a lattice gas model to model evacuation from a classroom [19]. On the other hand, a cellular automaton model has recently been used to study the best choice of exit doors location and width from a room without obstacles [21]. The aim of our paper is to consider the effect of obstacles in this problem. First, in Section 2 we describe the set of rules which govern the motion of pedestrians in the model, and in Section 3 some effects of the floor field choice on the simulation are briefly discussed. Then, in Section 4 we show that this model is able to reproduce at least qualitatively results observed in experiments and other models for empty rooms. Then, in Section 5 we apply the model to a classroom with regularly distributed desks and either one or two exits. Finally, in Section 6 we summarize the results and point out to future research.

## 2. Model description

In our model the room is described by a two-dimensional grid. Each cell can be empty, occupied by an obstacle or by a pedestrian. Its size corresponds to  $0.4 \times 0.4 \text{ m}^2$ , the typical surface occupied by a person in a dense situation [5]. Considering that mean velocity of pedestrians is around  $1 \text{ m/s}$  [5,19,21], moving  $0.4 \text{ m}$  per timestep  $\Delta t$  yields  $\Delta t \simeq 0.4 \text{ s}$ . Pedestrian dynamics is determined by (a) a static floor field, calculated so that motion towards the exit door is preferred, and by (b) interaction between persons. These features are described below.

### 2.1. Floor field

Once the geometry of the room and door location are determined, each cell is assigned a constant value representing its distance to the door. Lower values correspond to cells nearer the exit, and thus this static floor field indicates to the pedestrian the way to the exit, since they always prefer to move to a cell with a lower value than the current one.

The floor field is assigned as follows:

- (1) The room is divided in a rectangular grid. The exit door is assigned a value “1”.
- (2) Then all adjacent cells to the previous one (a “second layer” of cells) are assigned a value, according to the following rules:
  - (2.1) If a cell has value “ $N$ ”, then adjacent cells in the vertical or horizontal directions are assigned a value “ $N + 1$ ”. We will allow diagonal movements, thus it makes sense to consider adjacent cells in diagonal directions. We assign them a value “ $N + \lambda$ ”, with  $\lambda > 1$ . This is a simple attempt to represent the fact that the distance between two diagonally adjacent cells is larger than in horizontal or vertical directions. For this paper, we arbitrarily choose  $\lambda = \frac{3}{2}$ .
  - (2.2) If there are conflicts in the assignment of a value to a cell, because it is adjacent to cells with different floor fields, then the minimum possible value is assigned to the cell in conflict.
- (3) Then the third layer of cells is calculated, which is all cells adjacent to the second layer, and not in the first layer.
- (4) The process is repeated until all cells are evaluated.
- (5) Walls are also considered when defining the grid. Cells belonging to walls are given very high values of the floor field. This ensures that pedestrians will never attempt to occupy one of those cells.

Notice that the result is similar to the Manhattan metric, in the sense that the floor field at each cell is the minimum path length from an exit door to the cell. The difference lies in the fact that we allow diagonal

500	500	500	500	500	500	500	500	500	500	500	500	500	500	500	500	500	500	500	500	500	500
500	7.5	8	8.5	9	9.5	10	11	12	13	14	15	16	17	18	19	20	21	22	500		
500	6.5	7	7.5	8	8.5	9.5	10.5	11.5	12.5	13.5	14.5	15.5	16.5	17.5	18.5	19.5	20.5	21.5	500		
500	5.5	6	6.5	7	8	9	10	11	12	13	14	15	16	17	18	19	20	21	500		
500	4.5	5	5.5	6.5	7.5	8.5	9.5	10.5	11.5	12.5	13.5	14.5	15.5	16.5	17.5	18.5	19.5	20.5	500		
500	3.5	4	5	6	7	8	9	10	11	12	13	14	15	16	17	18	19	20	500		
500	2.5	3.5	4.5	5.5	6.5	7.5	8.5	9.5	10.5	11.5	12.5	13.5	14.5	15.5	16.5	17.5	18.5	19.5	500		
1	2	3	4	5	6	7	8	9	10	11	12	13	14	15	16	17	18	19	500		
1	2	3	4	5	6	7	8	9	10	11	12	13	14	15	16	17	18	19	500		
500	2.5	3.5	4.5	5.5	6.5	7.5	8.5	9.5	10.5	11.5	12.5	13.5	14.5	15.5	16.5	17.5	18.5	19.5	500		
500	3.5	4	5	6	7	8	9	10	11	12	13	14	15	16	17	18	19	20	500		
500	4.5	5	5.5	6.5	7.5	8.5	9.5	10.5	11.5	12.5	13.5	14.5	15.5	16.5	17.5	18.5	19.5	20.5	500		
500	5.5	6	6.5	7	8	9	10	11	12	13	14	15	16	17	18	19	20	21	500		
500	6.5	7	7.5	8	8.5	9.5	10.5	11.5	12.5	13.5	14.5	15.5	16.5	17.5	18.5	19.5	20.5	21.5	500		
500	7.5	8	8.5	9	9.5	10	11	12	13	14	15	16	17	18	19	20	21	22	500		
500	500	500	500	500	500	500	500	500	500	500	500	500	500	500	500	500	500	500	500	500	500

Fig. 1. Floor field for a room with  $18 \times 14$  cells. The exit door is at the left wall (cells with a value equal to 1); cells corresponding to walls are assigned a value of 500.

movements, and thus we need to consider diagonal movements when calculating the “distance” between the exit door and a cell.

Fig. 1 shows the floor field obtained by applying this set of rules to a room with an exit door on the left wall.

## 2.2. Movement and pedestrian interaction

At every iteration, each person must decide where to move. In our model, it always decides to move to the closest exit, that is, to the adjacent empty cell with the lowest floor field. Thus our model is in principle deterministic. We introduce three ways to make it non-deterministic:

- (1) If two or more neighboring cells have the same lowest floor field, a random number is used to decide the cell to which the person will intend to move.
- (2) If two pedestrians intend to move to the same cell, this conflict is decided by throwing a random number. The winner moves, the loser does not. This, and the fact that a pedestrian cannot move to an occupied cell, are the only interactions between pedestrians.
- (3) A certain amount of “panic” is introduced, given by a probability (5% in our model [21]) of the pedestrian to remain in his/her position even if he/she can move.

All these features are summarized in Fig. 2.

## 3. Simulation results: effect of chosen floor field

Given the above set of rules for floor field assignment and pedestrian movement, simulations can be performed. Fig. 3 shows a snapshot of a simulation.

Rule (2.1) for floor field assignment has the effect that a pedestrian would prefer to move diagonally towards the exit rather than in two consecutive and perpendicular steps, because the decrease in floor field is larger along a diagonal path. It is interesting to note the influence of this rule on the observed behavior of pedestrians in our simulations. In Fig. 4 we have the same room as in Fig. 3, but with  $\lambda = \infty$ . This means that diagonally adjacent cells are not considered when assigning the floor field to a cell. A snapshot of the simulation is shown. The corresponding floor field is shown in the Appendix, Fig. 18. It can be appreciated that, due to the floor field configuration, people accumulates along the diagonals heading to the door, in a very

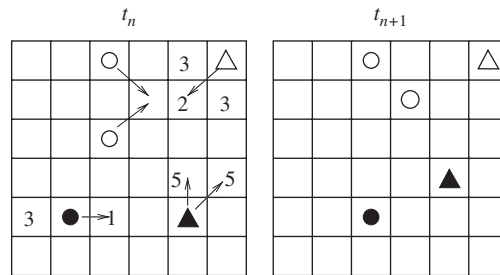


Fig. 2. Possible movements for pedestrians in our CA model. Numbers correspond to the floor field value in a cell, arrows to intended movements, and symbols to pedestrians in various situations. Filled circle: pedestrian moves to an adjacent cell to minimize floor field. Open circles: two pedestrians try to move to the same cell; a random number decides who moves. Filled triangle: two adjacent cells with equal floor field value, pedestrian decides randomly where to move. Open triangle: pedestrian in panic, does not move.

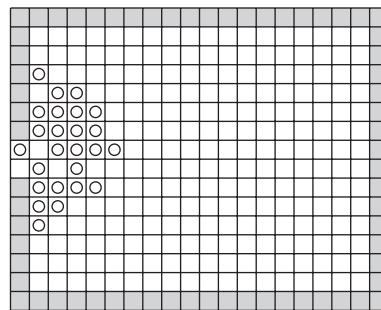


Fig. 3. Snapshot of a simulation with  $N = 50$  pedestrians, after 29 timesteps, in the floor field of Fig. 1. A semi-circular distribution of people forms at the exit.

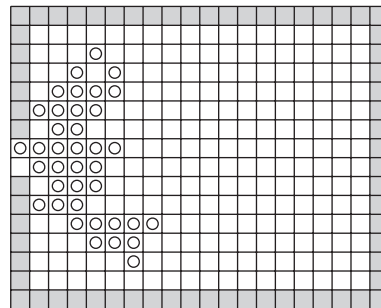


Fig. 4. Same as Fig. 3, but diagonal directions are not used to calculate the floor field ( $\lambda = \infty$ ). Snapshot of a simulation after 15 timesteps. The distribution of people is not semi-circular. Rather, it accumulates along two diagonals heading to the exit door.

unnatural distribution. [Figs. 3 and 4 correspond to different times in the evolution, but this does not affect conclusions. A configuration like Fig. 4 is not observed at any time if rule (2.1) is used.]

Thus, different (and, in principle, reasonable) choices of the floor field lead to behavior which is different not only quantitatively but also qualitatively, in contrast with some previous statements in the literature [22].

For completeness, we have also tested the usual Manhattan metric. The floor field and a typical snapshot are shown in Fig. 5. The distribution of people near the exit door is, again, clearly different. However, in this case the comparison is not precise, because when the Manhattan metric is used, diagonal motion is also not allowed, so the cellular automaton rules also change, and it is natural to expect a different behavior.

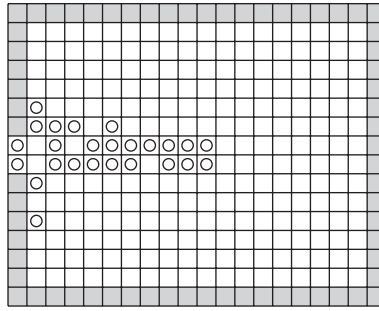


Fig. 5. Same as Figs. 1 and 3, but using the Manhattan metric. Snapshot of a simulation after 29 timesteps. The distribution of people is very different to Figs. 3 and 4.

#### 4. Simulation results: room without obstacles

In order to test our model we consider a room of  $14 \times 18$  cells, where  $N$  persons are initially distributed randomly. Room size and number of persons were chosen so as to be equivalent to those in Ref. [21]. An exit door of width  $a$  is placed at the center of the left wall (see, e.g., Figs. 3 and 4). The system is then iterated, and the evacuation time is calculated for various values of  $a$ . Actually, an average is calculated over 20 runs, each one differing only on the initial distribution of people (besides the random sequence of numbers associated to the panic variable and conflict resolution).

In Fig. 6 we plot the evacuation time (in timesteps units) versus exit width. Evacuation time decreases nonlinearly when  $a$  is increased, eventually reaching a saturation state where further increase in exit width does not have major effects on evacuation time. For the parameters chosen, such a critical value of the exit width is  $a \simeq 8$  (although it depends on  $N$  in general). These results are consistent with Ref. [21].

In principle, only initial configurations where no person is placed in the two rows closest to the door could be chosen, in order to prevent the premature occurrence of jamming [11]. However, for the geometry and number of persons studied in this paper, this is not a relevant effect. This is shown in Fig. 7. On average, evacuation times are in fact slightly shorter if no rows are prohibited, simply because people is initially nearer to the exit door. Anyway, time differences between both configurations are negligible, at least for the system under study, being not larger than  $5\Delta t \simeq 2$  s.

We can attempt to derive some simple scaling law to explain Fig. 6. Initially, all pedestrians are located at random positions occupying the whole room. In the simplest case, we can imagine all of them lining up in a single row from the exit door (see left panel of Fig. 8), assumed to be of width  $a = 1$ . In an ideal situation, where all movements are deterministic, and headed directly to the door, guided by the floor field, only the one closest to the door can move (labeled “1” in Fig. 8). Then, in the next step, both pedestrians “1” and “2” can move. Pedestrian “1” leaves the room and “2” advances one space. In the third step, pedestrians “2” and “3” move. The right panel of Fig. 8 shows a general intermediate situation. It is easy to show that the time needed to evacuate this row of  $N$  persons is  $2N$ . For a door of width  $a$ , we could line up  $a$  such rows, and the evacuation time would be

$$T \sim \frac{2N}{a}. \quad (1)$$

We can test this relation by plotting  $T/N$  for the data in Fig. 6. This is shown in Fig. 9, where also the proposed scaling  $2/a$  is plotted for comparison. For  $N > 100$  all data fall approximately on the same curve, although it is shifted with respect to Eq. (1). This could be due to the effect of collisions, non-rectilinear movement, and the “panic” variable, which increase the travel time with respect to the simple model in Fig. 8. For  $N = 50$ , however, the model clearly fails, maybe because, when density is low, the probability of moving without colliding with other pedestrian is less, and this strongly modifies the overall behavior, with respect to Fig. 8, where, in fact, at all times except for a few timesteps at the end of the evolution, there are interactions between pedestrians (by not allowing movement to an occupied cell).

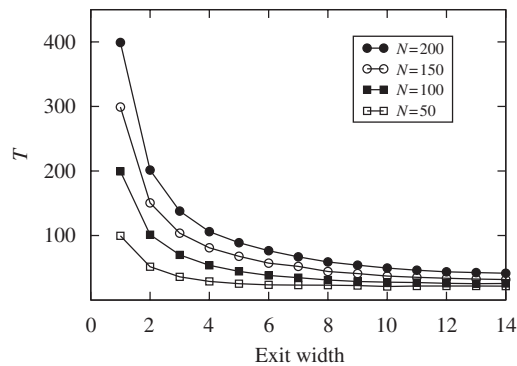


Fig. 6. Evacuation time  $T$  versus exit width for a  $14 \times 18$  room with a door located as in Fig. 3. Each curve corresponds to  $N = 200, 150, 100$ , and  $50$  occupants initially distributed at random.

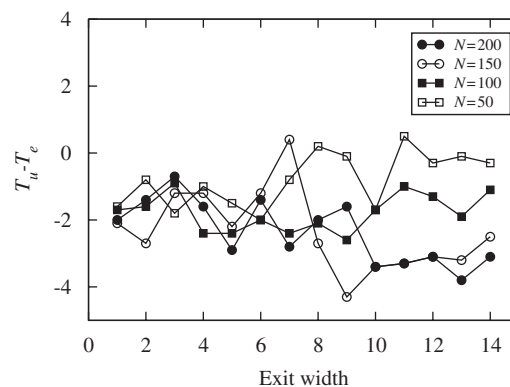


Fig. 7. Effect of leaving two rows unoccupied near the exit door in Fig. 3, to prevent premature jamming. Difference between the evacuation time when such rows are used in the initial configuration,  $T_u$ , and when they are empty,  $T_e$ , for all widths and initial number of persons used in Fig. 6. For each width, an average over 10 runs is plotted.

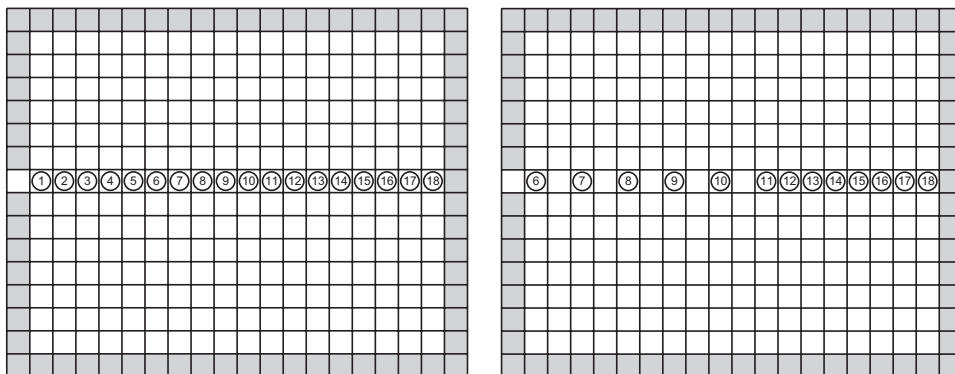


Fig. 8. Simple model to derive the scaling equation (1). Left panel: initial configuration, where all pedestrians line up to get out of the room through a door of width  $a = 1$ . Right panel: after a few timesteps, some pedestrians have exited, others can move forward, whereas others still cannot move because the cell in front of them is occupied.

## 5. Simulation results: room with obstacles

Obstacles are expected to modify the trajectory and therefore variables such as evacuation time or optimal width/placement of doors in a room. This modification can be quantified in our model by adequately recalculating

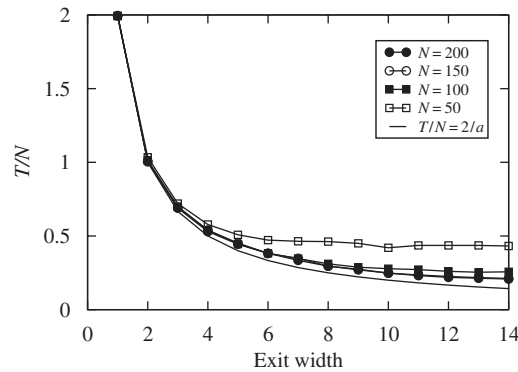


Fig. 9.  $T/N$  for the data in Fig. 6. The solid line corresponds to Eq. (1).

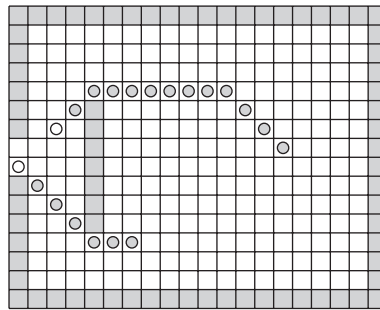


Fig. 10. Trajectory of two pedestrians in a  $14 \times 18$  room with a single obstacle in front of the exit door. The corresponding floor field is shown in the Appendix, Fig. 19. White (gray) circles indicate current (past) positions.

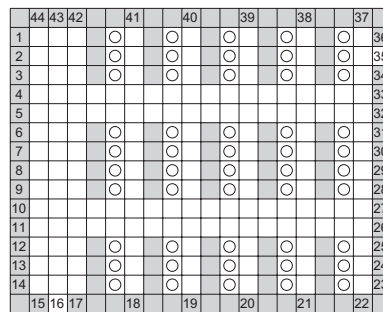


Fig. 11. Classroom of size  $14 \times 18$ , where 50 students are placed in their respective seats. White cells are empty cells, gray cells are walls/obstacles, and circles indicate the initial positions of the students. In this example there are two exit doors, at cells 16 and 35.

the floor field in the presence of obstacles. In our model, cells will be either empty, occupied by a pedestrian, or by an obstacle. When the floor field is calculated, obstacles are regarded as walls. In Fig. 10 we consider the same room as in Section 4, but with a single obstacle in front of the only exit. The result of a simulation with two persons is shown (the corresponding floor field is in the Appendix, Fig. 19). It can be seen that the floor field choice leads to a reasonable behavior of pedestrians in the model. Notice that this is achieved with a single static floor field, in contrast to other models where a complex geometry is dealt with by means of superposition of static fields [24].

For a given geometry and placement of the room, obstacles and exit doors, now we can distribute  $N$  persons in the room, and calculate the evacuation time. In this paper we consider a classroom (see Fig. 11).

As shown in Fig. 11, it consists of a certain number of desks. Behind each desk there is a student. We consider either two single doors or one double door, where a single (double) door is such that one (two) persons can leave the room through it simultaneously. We perform a series of runs on this system, modifying the position of the exit door(s) in order to determine its optimum location.

First, for a unique exit door, we study the effect of obstacles in the optimum location for the door. Fig. 12 shows evacuation times for a classroom without obstacles (open circles) and with obstacles (filled circles), for different door locations. To single out the effect of obstacles, persons are located in the same places, even if there are no desks. This causes the sharp transition between the door being located in the right wall and in the side and back walls. It is simply an effect of the pedestrians being nearer or farther from the exit door on average. Another effect is the dip which forms when the door is located in cells 18–22 (labeled in Fig. 11), if desks are present. We can guess that the presence of an aisle next to the exit door is a favorable situation, as it coordinates pedestrian motion, avoiding interactions, which in turn leads to lower evacuation times. This is consistent with Fig. 9, where the simple model of a single row (see Fig. 8) underestimates the evacuation time, and with Fig. 15.

We have also analyzed the effect of obstacles in the optimum width for an exit door located at the center of the left wall. In Fig. 13, open circles correspond to evacuation times for the classroom if no obstacles are present, and filled circles to evacuation times for the classroom with desks. We see that the critical value for which further increase of door width does not noticeably increase evacuation time, is lower with obstacles present (around 8 without obstacles, and 4 with obstacles), and that the transition is sharper. In this case, increasing the exit width beyond  $a = 4$  does not make any difference, since the presence of obstacles imposes constraints on the motion of pedestrians (by creating aisles of fixed width) which are locally more important.

A common setting in classrooms is to have double doors, that is, doors where two persons can pass simultaneously. Results are plotted in Fig. 14.

We notice that the worst case (highest evacuation time) occurs when the exit is at the corners of the room (occupying cells 16 and 17), and that the optimal situation is when the door is at the back of the room (occupying cells 29 and 30). In the latter case, evacuation time is  $51.4 \pm 0.5\Delta t$  (error estimated with the average

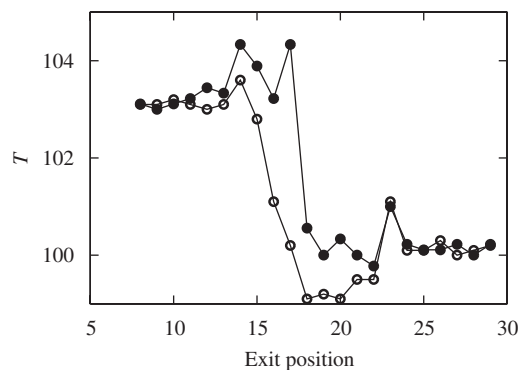


Fig. 12. Evacuation time for  $N = 50$  seated students in the classroom of Fig. 11 with (filled circles) and without (open circles) obstacles, for varying door location. An average over 10 runs for each door location is plotted. Door locations are labeled as in Fig. 11.

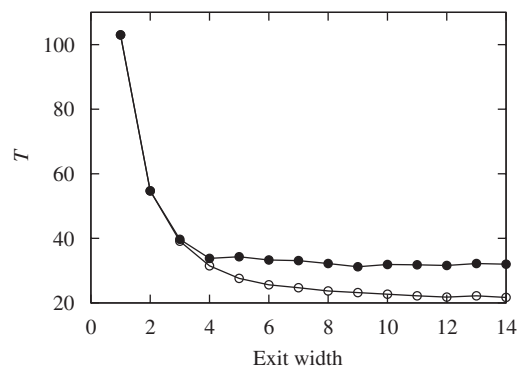


Fig. 13. Evacuation time for the classroom in Fig. 11 with (filled circles) and without (open circles) obstacles, for increasing door width.



deviation of data from the mean value). This corresponds to about 20 s, which is a reasonable result. It is interesting that the highest evacuation time (labeled *b* in Fig. 14) is obtained for a rather traditional location of the exit door in a classroom with this distribution of desks. Another traditional location is at the front wall. It corresponds to the point labeled *a* in Fig. 14. Evacuation times are much better, around 15% less.

Next, we replace the double door by two single doors. Fig. 15 shows the locations of both doors which minimize evacuation time. The best results are, thus, when doors are at the sides of the room, which resembles results for similar geometries [24]. The best exit time is  $49.8 \pm 0.8\Delta t$ . Thus, two single doors are slightly better than one double door.

We have repeated some of the calculations above for a more densely occupied classroom (see Fig. 16). Evacuation time versus exit position is plotted in Figs. 17(a) (single door) and (b) (double door).

## 6. Summary

In this paper, a bidimensional cellular automaton model was used to simulate an evacuation process from a room with and without obstacles, following the work of Daoliang et al. [21]. Given a room geometry and a distribution of obstacles, a floor field is calculated for each cell. The floor field is such that pedestrians head to the exit door by moving to an empty cell with the lowest floor field. A “panic” variable is introduced, given

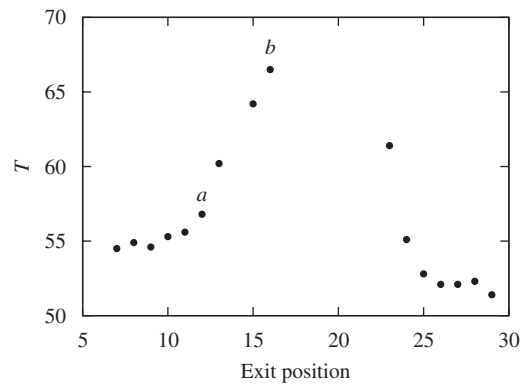


Fig. 14. Evacuation time from the classroom in Fig. 11 for all possible positions of a double door. A point with abscissa *n* corresponds to a double door occupying cells *n* and *n* + 1, as labeled in Fig. 11. Notice that some locations are impossible (not enough space for a double door). Two traditional locations to place such a door have been labeled *a* (occupying cells 12–13) and *b* (at cells 16–17).

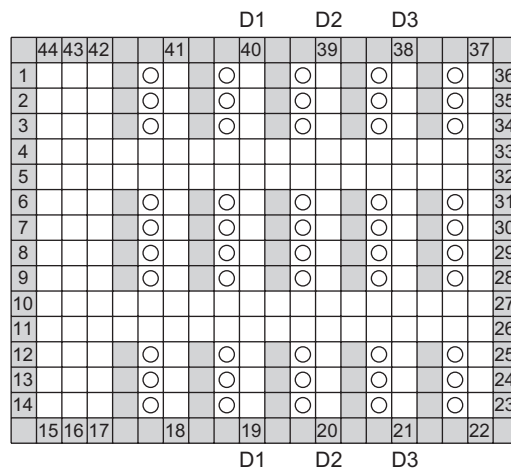


Fig. 15. Diagram of the classroom in Fig. 11, with two single exit doors. The best locations for the couple of doors are marked in the figure (D1, D2, D3, in decreasing order of evacuation time).

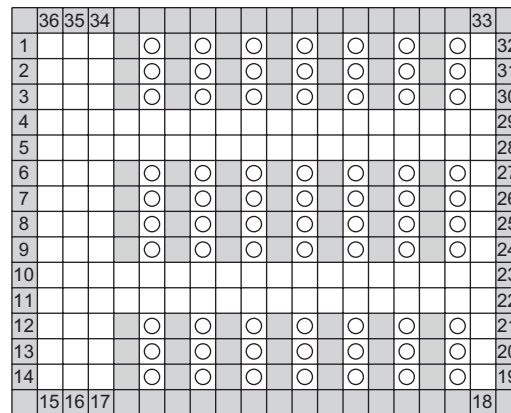


Fig. 16. A classroom more densely occupied than Fig. 11. There is only space for a single pedestrian between desks, so  $N = 70$  (instead of 50) persons are inside.

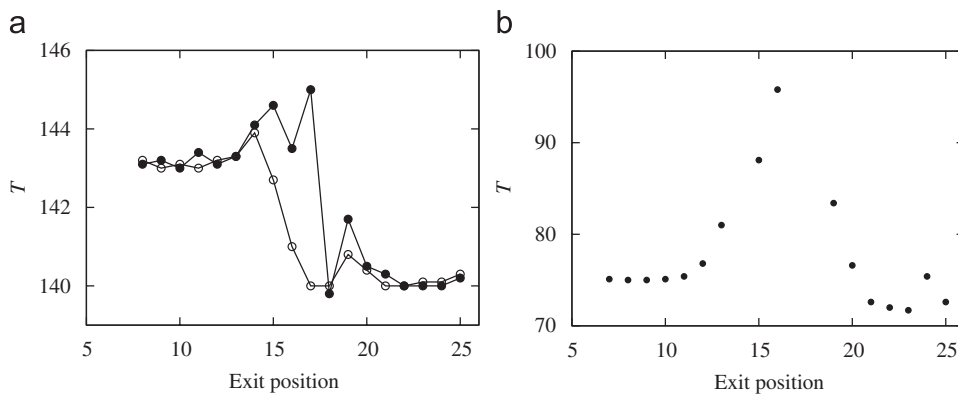


Fig. 17. Evacuation time versus exit position for the classroom in Fig. 16, with (filled circles) and without (open circles) obstacles: (a) single door; (b) double door.

by a 5% probability of not moving. Also, when pedestrian motions are in conflict, they are resolved by a random choice. These features make the model non-deterministic. For comparison with previous works, a room without obstacles is considered, obtaining known features like arching at the exit [5,12,23] and the existence of a critical value for the exit door width, such that increasing width does not improve evacuation times [21].

Then the model is used to study evacuation from a classroom at full capacity. Two types of doors are considered: single (where only one person can pass through the door) and double doors (where two persons can pass simultaneously). For a unique single door, evacuation times with and without obstacles were compared, for varying door position and width. For varying width, it is found that the critical value, beyond which increasing width does not decrease evacuation times, is lower with obstacles. For a double exit door, the optimum position, where evacuation time is minimized, is at the back of the room. A traditional position, at one of the corners, turns out to yield the worst evacuation time. If the double door is replaced by two single doors, evacuation times are only slightly decreased.

Certainly, there are several features which can be improved in the model. For instance, obstacles in the model can only occupy an integer number of cells (see Figs. 10 and 11). This is not true in general, and could be addressed by reducing cell size. However, results are expected to be qualitatively correct [25]. Also, chairs have been ignored in Fig. 11, and this is another source of obstacles which deserves to be considered. In fact, chairs could be considered as a movable obstacle, and this is an interesting modification to the model worth investigating. Finally, there is the parameter  $\lambda$  introduced in Section 2.1, to weight the increase in floor field for diagonally adjacent cells. In this work we arbitrarily chose  $\lambda = \frac{3}{2}$ , and made some calculations with  $\lambda = \infty$  (Fig. 4), but it would be interesting to examine the effects of  $\lambda$  in the evolution of pedestrians. However, there

are many other effects we have ignored in this model, like kin behavior [18] and competitive/cooperative behavior [14], a personal tendency in each pedestrian to follow/avoid crowds, etc., effects which can be modeled by a non-static floor field and may turn out to be more important than the precise choice of  $\lambda$ .

We intend to address some of these and other issues (like applying the model to other geometries of interest, such as movie theaters, stadiums, etc.) in future work.

## Acknowledgments

This project has been financially supported by FONDECYT under contracts No. 1070854 (JAV), No. 1070131 (JAV), No. 1070080 (JR), No. 1071062 (JR), No. 1060830 (VM), and No. 3060029 (BT).

## Appendix A. Floor fields

In this appendix, we show the floor fields used to run some of the simulations presented in the text (see Figs. 18 and 19).

500	500	500	500	500	500	500	500	500	500	500	500	500	500	500	500	500	500	500	500	500
500	7	7	7	7	7	7	8	9	10	11	12	13	14	15	16	17	18	19	500	500
500	6	6	6	6	6	7	8	9	10	11	12	13	14	15	16	17	18	19	500	500
500	5	5	5	5	6	7	8	9	10	11	12	13	14	15	16	17	18	19	500	500
500	4	4	4	5	6	7	8	9	10	11	12	13	14	15	16	17	18	19	500	500
500	3	3	4	5	6	7	8	9	10	11	12	13	14	15	16	17	18	19	500	500
500	2	3	4	5	6	7	8	9	10	11	12	13	14	15	16	17	18	19	500	500
1	2	3	4	5	6	7	8	9	10	11	12	13	14	15	16	17	18	19	500	500
1	2	3	4	5	6	7	8	9	10	11	12	13	14	15	16	17	18	19	500	500
500	2	3	4	5	6	7	8	9	10	11	12	13	14	15	16	17	18	19	500	500
500	3	3	4	5	6	7	8	9	10	11	12	13	14	15	16	17	18	19	500	500
500	4	4	4	5	6	7	8	9	10	11	12	13	14	15	16	17	18	19	500	500
500	5	5	5	5	6	7	8	9	10	11	12	13	14	15	16	17	18	19	500	500
500	6	6	6	6	6	7	8	9	10	11	12	13	14	15	16	17	18	19	500	500
500	7	7	7	7	7	7	8	9	10	11	12	13	14	15	16	17	18	19	500	500
500	500	500	500	500	500	500	500	500	500	500	500	500	500	500	500	500	500	500	500	500

Fig. 18. Floor field for the simulation in Fig. 4.

500	500	500	500	500	500	500	500	500	500	500	500	500	500	500	500	500	500	500	500	500
500	7.5	8.0	8.5	9.0	9.5	10	11	12	13	14	15	16	17	18	19	20	21	22	500	500
500	6.5	7.0	7.5	8.0	8.5	9.5	10.5	11.5	12.5	13.5	14.5	15.5	16.5	17.5	18.5	19.5	20.5	21.5	500	500
500	5.5	6	6.5	7	8	9	10	11	12	13	14	15	16	17	18	19	20	21	500	500
500	4.5	5	5.5	6.5	7.5	8.5	9.5	10.5	11.5	12.5	13.5	14.5	15.5	16.5	17.5	18.5	19.5	20.5	500	500
500	3.5	4	5	500	8	9	10	11	12	13	14	15	16	17	18	19	20	21	500	500
500	2.5	3.5	4.5	500	9	9.5	10.5	11.5	12.5	13.5	14.5	15.5	16.5	17.5	18.5	19.5	20.5	21.5	500	500
1	2	3	4	500	10	10.5	11	12	13	14	15	16	17	18	19	20	21	22	500	500
1	2	3	4	500	11	11.5	12	12.5	13.5	14.5	15.5	16.5	17.5	18.5	19.5	20.5	21.5	22.5	500	500
500	2.5	3.5	4.5	500	10.5	11	11.5	12.5	13.5	14.5	15.5	16.5	17.5	18.5	19.5	20.5	21.5	22.5	500	500
500	3.5	4	5	500	9.5	10	11	12	13	14	15	16	17	18	19	20	21	22	500	500
500	4.5	5	5.5	500	8.5	9.5	10.5	11.5	12.5	13.5	14.5	15.5	16.5	17.5	18.5	19.5	20.5	21.5	500	500
500	5.5	6	6.5	7	8	9	10	11	12	13	14	15	16	17	18	19	20	21	500	500
500	6.5	7.0	7.5	8.0	8.5	9.5	10.5	11.5	12.5	13.5	14.5	15.5	16.5	17.5	18.5	19.5	20.5	21.5	500	500
500	7.5	8.0	8.5	9.0	9.5	10	11	12	13	14	15	16	17	18	19	20	21	22	500	500
500	500	500	500	500	500	500	500	500	500	500	500	500	500	500	500	500	500	500	500	500

Fig. 19. Floor field for the simulation in Fig. 10.

## References

- [1] D. Helbing, Traffic and related self-driven many-particle systems, *Rev. Mod. Phys.* 73 (4) (2001) 1067–1141.
- [2] T. Nagatani, The physics of traffic jams, *Rep. Prog. Phys.* 65 (9) (2002) 1331–1386.
- [3] D. Chowdhury, L. Santen, A. Schadschneider, Statistical physics of vehicular traffic and some related systems, *Phys. Rep.* 329 (4–6) (2000) 199–331.
- [4] B.A. Toledo, V. Muñoz, J. Rogan, C. Tenreiro, J.A. Valdivia, Modeling traffic through a sequence of traffic lights, *Phys. Rev. E* 70 (1) (2004) 016107.
- [5] C. Burstedde, K. Klauck, A. Schadschneider, J. Zittartz, Simulation of pedestrian dynamics using a two-dimensional cellular automaton, *Physica A* 295 (2001) 507–525.
- [6] D. Helbing, P. Molnár, Social force model for pedestrian dynamics, *Phys. Rev. E* 51 (5) (1995) 4282–4286.
- [7] M. Muramatsu, T. Irie, T. Nagatani, Jamming transition in pedestrian counter flow, *Physica A* 267 (1999) 487–498.
- [8] M. Muramatsu, T. Nagatani, Jamming transition in two-dimensional pedestrian traffic, *Physica A* 375 (2000) 281–291.
- [9] Y. Tajima, T. Nagatani, Clogging transition of pedestrian flow in T-shaped channel, *Physica A* (2002) 239–250.
- [10] M. Muramatsu, T. Nagatani, Jamming transition of pedestrian traffic at a crossing with open boundaries, *Physica A* 286 (2000) 377–390.
- [11] G.J. Perez, G. Tapang, M. Lim, C. Saloma, Streaming, disruptive interference and power-law behavior in the exit dynamics of confined pedestrians, *Physica A* 312 (2002) 609–618.
- [12] D. Helbing, I. Farkas, T. Vicsek, Simulating dynamical features of escape panic, *Nature* 407 (2000) 487–490.
- [13] M. Isobe, D. Helbing, T. Nagatani, Experiment, theory, and simulation of the evacuation of a room without visibility, *Phys. Rev. E* 69 (2004) 066132.
- [14] A. Kirchner, H. Klüpfel, K. Nishinari, A. Schadschneider, M. Schreckenberg, Simulation of competitive egress behavior: comparison with aircraft evacuation data, *Physica A* 324 (2003) 689–697.
- [15] F. Weifeng, Y. Lizhong, F. Weicheng, Simulation of bi-direction pedestrian movement using a cellular automata model, *Physica A* 321 (2003) 633–640.
- [16] W.G. Weng, T. Chen, H.Y. Yuan, W.C. Fan, Cellular automaton simulation of pedestrian counter flow with different walk velocities, *Phys. Rev. E* 74 (2006) 036102.
- [17] Y. Tajima, K. Takimoto, T. Nagatani, Scaling of pedestrian channel flow with a bottleneck, *Physica A* 294 (2001) 257–268.
- [18] L.Z. Yang, D. Zhao, J. Li, T.Y. Fang, Simulation of the kin behavior in building occupant evacuation based on cellular automaton, *Build. Environ.* 40 (2005) 411–415.
- [19] D. Helbing, M. Isobe, T. Nagatani, K. Takimoto, Lattice gas simulation of experimentally studied evacuation dynamics, *Phys. Rev. E* 67 (2003) 067101.
- [20] Y. Tajima, T. Nagatani, Scaling behavior of crowd flow outside a hall, *Physica A* 292 (2001) 545–554.
- [21] Z. Daoliang, Y. Lizhong, L. Jian, Exit dynamics of occupant evacuation in an emergency, *Physica A* 363 (2005) 501–511.
- [22] A. Kirchner, A. Schadschneider, Simulation of evacuation processes using a bionics-inspired cellular automaton model for pedestrian dynamics, *Physica A* 312 (2002) 260–276.
- [23] S. Wei-Guo, Y. Yan-Fei, W. Bing-Hong, F. Wei-Cheng, Evacuation behaviors at exit in CA model with force essentials: a comparison with social force model, *Phys. A* 371 (2006) 658–666.
- [24] C. Burstedde, A. Kirchner, K. Klauck, A. Schadschneider, J. Zittartz, Cellular automaton approach to pedestrian dynamics—applications, in: M. Schreckenberg, S. Sharma (Eds.), *Pedestrian and Evacuation Dynamics*, Springer, Berlin, 2001, p. 87.
- [25] A. Kirchner, H. Klüpfel, K. Nishinari, A. Schadschneider, M. Schreckenberg, Discretization effects and the influence of walking speed in cellular automata models for pedestrian dynamics, *J. Stat. Mech.* 10 (2004) P10011.